The efficiency of individual optimization in the conditions of competitive growth

J. Kočišová [1], D. Horváth [1,2,3] B. Brutovský [1]

[1] *Institute of Physics, Faculty of Science, P. J. Šafárik University, Park Angelinum 9, 041 54 Košice, Slovakia*

[2] *Centre de Biophysique Moléculaire, CNRS; Rue Charles Sadron, 45071 Orléans, France*

[3] *Department of Physics, Faculty of Electrical Engineering and Informatics, Technical University, Letná 9, 042 00 Košice*

Abstract

The paper aims to discuss statistical properties of the multi-agent based model of competitive growth. Each of the agents is described by growth (or decay) rule of its virtual "mass" with the rate affected by the interaction with other agents. The interaction depends on the strategy vector and mutual distance between agents and both are subjected to the agent's individual optimization process. Steady-state simulations yield phase diagrams with the high and low competition phases (HCP and LCP, respectively) separated by critical point. Particular focus has been made on the indicators of the power-law behavior of the mass distributions with respect to the critical regime. In this regime the study has revealed remarkable anomaly in the optimization efficiency.

Key words: growth model, agent-based systems, optimization
PACS: 89.65.-s, 87.55.de, 05.70.Jk, 89.75.Fb

1 Introduction

Competitive growth [1] is one of the most generic processes observable in wide range of spatiotemporal scales. The rate of the growth/decay of the quantity $M(t)$ which represents some "virtual mass" of the object might be defined by the first-order continuous dynamics

$$\frac{\mathrm{d}M}{\mathrm{d}t} = Rate(M) = Growth(M) - Decay(M)\,. \tag{1}$$

Email address: jana.kocisova@kosice.upjs.sk (J. Kočišová [1]).

Here the $Decay(M)$ which contributes into overall $Rate(M)$ comprises many possible processes such as death, destruction, slowering due to competition. Most of the baseline studies start from the logistic rate form [2,3]. This minimum model includes the Malthusian term $Growth(M) = \alpha_{\rm m} M$, $\alpha_{\rm m} > 0$ and specific quadratic term

$$Decay(M) = \frac{M^2}{M_{\rm c}}\,, \tag{2}$$

where the competition is quantified by the *carrying capacity* [4] denoted as $M_{\rm c}$. Despite the logistics is well known since early studies of growth processes, for our purposes several comments regarding its structure will be helpful. As $M(t)$ approaches $M_{\rm c}$ for $\alpha_{\rm m} > 0$ the growth slows down until $Rate(M_{\rm c}) = 0$. The ability to detect or even quantify the proximity of mass saturation may be invaluable in a broad variety of the real world applications, enabling one to avoid the saturation. The rate reduction of the type $1 - M/M_{\rm c}$ has been used for mathematical description of tumor growth at tissue level [5] as well as cellular scales [2,5,6]. At the model level, the proximity of carrying capacity may stimulate growing entities to optimize their instant conditions. One can say that individual optimization [7,8] raises as coevolutionary mechanism preventing competitors from the imposed obstructions [1].

In the present paper we analyze statistical efficiency of optimization process of growing entities under the competitive conditions, where agent may change the strategy or migration routing to the more perspective regions by optimization. This goal requires much more detailed comprehensive and spatially distributed model than the logistic equation is, nevertheless, simple principles of logistic bounding and growth can be incorporated into construction of multiple entities called autonomous agents. The agent-based paradigm [9,10] states that even relatively simple rules may lead to very complex emergent behavior. Many examples may be found, but for brevity we mention only few of them: organizations of insect colonies [11,12], social [13], human economic behavior [10] or firms as autonomous entities [14].

The abstract agent-based model producing emergent "mass" distributions is presented in this paper. The interpretation of $M(t)$ or virtual "mass" itself depends on the scale and application field for which the model has been suggested. Here, the scalar can represent the variety of possible quantities, such as length or size of an organism, but also diameter or volume of the growing bacterial colony. We assume that the model can be helpful also in the study of generic features at economic and social scales. In this frame $M(t)$ may represent wealth [15] of single seller, personal income [16], money owned by citizens [17], firm size [18]. From the standpoint of the total mass behavior one can, in principal, distinguish between the models that conserve mass [17] and models that violate this type of invariance. As non-conservativeness may be understood as a synonym for incompleteness or

missing information about all of the existing mass flows, it may be also understood as a realistic feature of the growth and mass-exchange models. Our focus on fluctuations is in part motivated by the effort to understand the origins of *power-law distributions* [15,16,17,18,19,20] in the systems which exhibit signs of the growth and competition [1,21].

In the economic context the interest dates back to the seminal Pareto's work [22]. General formulation of the problem is motivated by the fact that power-law distributions also known as Zipf's law [23,19] found also in distributions of city size [19]. The power-law distribution can be identified in the lifetimes [24], earthquake distributions [25], firm demises [14] or size of spatial colonies [26] as well. Here presented agent-based simulations contribute to the discussion about connection of power-law distributions with critical regime of driving parameters. This idea, stimulated by the concept of the feedback [27] and self-organized criticality [28,25,24], has been revisited in [29].

The structure of this paper will be as follows. In Section 2 we introduce agent-based model of the reactive interacting agents which manifests growth within the mass inequality constraints. Moreover, the agents are able to optimize their strategies and positions (see subsec. 2.3). In Section 3 statistical characteristics obtained by the numerical simulations are discussed. These results open the question about the role of the local individual optimization. Finally, the concluding remarks and perspectives of our approach are presented.

2 The agent-based model

In the paper, we incorporate mechanisms of growth, individual search and competetivness into the continuous stochastic agent-based framework and analyze equilibrium statistical consequences of the complex model. Below we present model in more detailed focus now.

2.1 State of agent

The system consisting of N interacting autonomous agents, each of them equipped with specific abilities, is considered. It represents sufficiently complex and general model, where the formation and growth phenomena are interrelated with space, strategic and mobility issues of the competitive world. At time t, the state of ith agent is described by the tuple $\langle \mathbf{X}_i^{(t)}, \mathbf{S}_i^{(t)}, M_i^{(t)} \rangle$, where $\mathbf{X}_i^{(t)}$ is the position, $\mathbf{S}_i^{(t)}$ the strategy and $M_i^{(t)}$ the mass of ith agent, respectively. The spatial coordinates are

taken from real space

$$\mathbf{X}_i^{(t)} = \left[X_{i,1}^{(t)}, X_{i,2}^{(t)}, \ldots, X_{i,d_{\mathrm{x}}}^{(t)} \right] , \quad X_{i,l}^{(t)} \in \langle 0, L \rangle \, . \tag{3}$$

The state of agent is characterized by the abstract vector of strategy

$$\mathbf{S}_i^{(t)} = \left[S_{i,1}^{(t)}, S_{i,2}^{(t)} , \ldots S_{i,d_{\mathrm{s}}}^{(t)} \right] , \qquad S_{i,k}^{(t)} \in \langle 0, 1 \rangle \, . \tag{4}$$

considered with normalization

$$\| \, \mathbf{S}_i^{(t)} \, \| \equiv \sqrt{\sum_{k=1}^{d_{\mathrm{s}}} \left(S_{i,k}^{(t)} \right)^2} = 1 \, . \tag{5}$$

Here $\mathbf{S}_i^{(t)}$ defines the relative importance of the particular strategies, but the amplitude of their pursuing is determined by the mass (see in subsec. 2.2). The strategic vector is defined as an abstract information carrier which determines the strength of inter-agent interaction. In what follows, we use $d_{\mathrm{x}} = 2$ and $d_{\mathrm{s}} = 10$.

2.2 Growth mass rules

In analogy with logistic growth, the mass of each agent is considered to evolve according to discrete dynamics as it follows

$$M_i^{(t+1)} = \alpha M_i^{(t)} - \beta \Omega_i^{(t)} \, . \tag{6}$$

Here α is the constant growth rate parameter and β the feedback parameter. Generally, the second term $(-\beta \Omega_i^{(t)})$ describes the effect of pairwise competition. In further, we consider the regime with $\alpha > 1$. In that case a discrete model incorporates the growth property.

The competitive term in Eq.(6) is based on the overlap

$$\Omega_i^{(t)} \equiv \Omega(\mathbf{X}_i^{(t)}, \mathbf{S}_i^{(t)}) = \sum_{i \neq j}^{N} J_{i,j}^{(t)} \sum_{k=1}^{d_{\mathrm{s}}} S_{i,k}^{(t)} S_{j,k}^{(t)} \tag{7}$$

weighted by the pair-wise real-space distance matrix

$$J_{i,j}^{(t)} = J \frac{M_i^{(t)} \, M_j^{(t)}}{\left(\| \, \mathbf{X}_i^{(t)} - \mathbf{X}_j^{(t)} \, \|^2 + \epsilon^2 \right)^{\gamma/2}} \, , \tag{8}$$

which takes into account actual positions of agents. The tensorial structure $M_i^{(t)}\, M_j^{(t)}$ has been chosen in analogy to scalar form of decay outlined by Eq.(2). An important feature of agents is their ability to perform transformation of scalar nourishment αM_i into "vector mass" $M_i \mathbf{S}_i$ diversified by the components of $\mathbf{S}_i$. In this context it has to be reminded that growing mass increases the impact of the respective strategy on the dynamics of its neighbors. Quite analogously as in the logistic function, we define the pairwise interaction to be proportional to the product of virtual masses and interaction parameter J. At the large inter-agent distances interaction turns to the asymptotics $\propto M_i^{(t)} M_j^{(t)} \|\mathbf{X}_i^{(t)} - \mathbf{X}_j^{(t)}\|^{-\gamma}$. For the small distances, the parameter ϵ is introduced to prevent from the proximity effects. The chosen form of the inter-agent pair interactions is of the short-range type (γ, see in Tab. 1), spherically symmetric and purely repulsive.

2.3 Optimization as a individual coevolutionary mechanism in dynamic landscape

The optimization starts by the analysis of external stimuli represented by actual Ω_i. In general, individual optimization is the coevolutionary mechanism which serves to adapt to local competitive dynamical environment [30,9] understood as formed by the surrounding agents.

In our model, the optimization of $\Omega_i^{(t)} \equiv \Omega\left(\mathbf{X}_i^{(t)}, \mathbf{S}_i^{(t)}\right)$ is considered to be the cause of the motion in the coordinate and strategic spaces. Here we use the *hill climbing* optimization technique which is the standard component of agent-based modeling [9]. The expected consequence of the optimization is weakening of the competition pressure on i-th agent. According to Eq.(6) smaller Ω_i leads to slower loss of the mass in onward iterations. The optimization of the selected agent is applied with probability P_{opt}. Technically, in the simulation process the optimization is accepted if P_{opt} becomes larger than random number drawn uniformly from $(0, 1)$. When the step is accepted, the agent has to decide among two alternatives: positional or strategy optimization. The individual optimization process which claims to find better position

$$\mathbf{X}_i^{(t+1)} = \hat{H}\left(\mathbf{X}_i^{(t)}, N_{\mathrm{H}}, \delta_{\mathrm{x}}^{(t)}\right) \tag{9}$$

is accepted with probability P_{ps}. Here $\hat{H}$ denotes the hill climbing operator characterized by N_{H} variable displacements $\delta_{\mathrm{x}}^{(t)}$. The iterations of strategic optimization formally written as

$$\mathbf{S}_i^{(t+1)} = \hat{H}\left(\mathbf{S}_i^{(t)}, N_{\mathrm{H}}, \delta_{\mathrm{s}}^{(t)}\right) \tag{10}$$

are accepted with probability $1 - P_{\mathrm{ps}}$.

At first, Let as focus on the spatial optimization in more details. Formally, $\hat{H}$ applied to the search for optimal coordinates $\mathbf{X}_i$ has been decomposed into particular tasks solved by the sub-operators

$$\mathbf{X}_{i,(n)}^{(t)} = \hat{H}_{\mathrm{sub}}\left(\mathbf{X}_{i,(n-1)}^{(t)}, \delta_{\mathrm{x}}^{(t)}\right) , \qquad n = 1, 2, 3, \ldots, N_{\mathrm{H}} , \tag{11}$$

where $\mathbf{X}_{i,(0)}^{(t)} = \mathbf{X}_i^{(t)}$ represents initial coordinates for the optimization process. For each of N_{H} steps we perform the calculation of corresponding Ω_i for actual trial coordinates. It consists of calculation of $J_{i,j}$ matrix and overlap by means of Eq.(7) and Eq.(8). For kth spatial coordinate, and nth application of Eq.(11) we suppose the trial move

$$X_{i,k,(n)}^{(t),\mathrm{trial}} = X_{i,k,(n-1)}^{(t)} + \delta_{\mathrm{x}}^{(t)}\left(2\xi_{i,k,(n-1)}^{(t)} - 1\right) , \tag{12}$$

where $\xi_{i,k,(n-1)}^{(t)}$ is a random number drawn from a uniform distributions $(0, 1)$. The agent-based system is not conservative, but its square boundaries are impenetrable by mass. The agents must restrict their moves within boundaries, and thus path corrections are needed for $X_{i,k,(n)}^{(t),\mathrm{trial}}$.

The optimization uses two alternative displacements [1]: $\delta_{\mathrm{x}}^{(t)} \in \{\delta_{\mathrm{x}_1}, \delta_{\mathrm{x}_2}\}$, where $\delta_{\mathrm{x}_1} > \delta_{\mathrm{x}_2}$. The larger step δ_{x_1} is drawn with probability P_{big}. The dichotomy of steps has intuitive reasons supported by the preliminary simulations. The step size δ_{x_1} can be efficient to find location in the remote areas, whereas the displacement δ_{x_2} helps to refine the spatial positions.

The constant (spatially uniform) α in model does not guarantee automatically uniform access to external resources as the free boundary conditions are imposed. The character of interactions combined with given conditions brings permanent heterogeneity in the access to external sources. The nonequivalent persistent nonuniformities at corners and edges can be in particular overcome by considering sufficiently large systems and short-range interactions. Formally, the optimization consists of the sequence of particular decisions given by

$$\begin{aligned} &\textbf{if} \quad \Omega\left(\mathbf{X}_{i,(n)}^{(t),\mathrm{trial}}, \mathbf{S}_i^{(t)}\right) \leq \Omega\left(\mathbf{X}_{i,(n-1)}^{(t)}, \mathbf{S}_i^{(t)}\right) \\ &\qquad \textbf{then} \quad \mathbf{X}_{i,(n)}^{(t)} = \mathbf{X}_{i,(n)}^{(t),\mathrm{trial}} \quad \textbf{otherwise} \quad \mathbf{X}_{i,(n)}^{(t)} = \mathbf{X}_{i,(n-1)}^{(t)} . \end{aligned} \tag{13}$$

When $n = N_{\mathrm{H}}$ the output of individual optimization $\mathbf{X}_i^{(t+1)} = \mathbf{X}_{i,(N_{\mathrm{H}})}^{(t)}$ is achieved [see Eq. (9)].

The analogous procedure which uses two different types of steps δ_{s_1}, δ_{s_2} is assumed for the optimization of $\mathbf{S}_i$. The only exception is the normalization of the strategy vector [see Eq.(5)] which has to be applied after each optimization move.

The above presented agent-based model shares many features with bacterial species optimizing their access to nutrients in different conditions [31]. In this context the identification of Ω_i is analogous to output of bacterial chemosensory system and the decision from the optimization can be the switching between staying in the same or moving to better place.

2.4 Mass constraints, birth/death processes

The iterative scheme Eq.(6) fails to describe mass dynamics when passing to extremal values of masses. This deficiency of the model must be eliminated by additional constraints and limitations. We have considered the mass bounded by the lower cutoff, $M_{\rm d}$. If, due to competition, the mass has decreased bellow $M_{\rm d}$, the agent is replaced by a new one in random initial state. The situation may be interpreted as death or crash. As the number of agents is conserved, the death of one agent opens the playground for immediate birth of his descendant with parameters drawn in a random way, analogously as in the stage of initialization (i.e. with initial mass equal to $2\,M_{\rm d}$). The operating near threshold $M_{\rm d}$ yields ergodicity gain in a way of extremal dynamics [28], which avoids from getting stuck.

Preliminary numerical simulations uncovered that there remains specific issue unresolved related to nonstationarity of mass distributions [32] caused by the growth very weighty agents. More profound analysis showed that quadratic form $M_i M_j$ involved in Eq.(8) might not stop the growth if the masses of competing neighbours are not sufficiently high. Stationarity may be reached by introducing upper mass cutoff $M_{\rm up}$. By the update $M_i^{(t)} \leftarrow M_{\rm up}$ the agent suddenly reacts to the situation $M_i^{(t)} > M_{\rm up}$. This limitation can be understood as an extra constraint which guarantees renewability of sources. In the economic context the introducing of $M_{\rm up}$ may roughly represent very restrictive taxation system.

3 Results

During the assembly preparation, the positions $\mathbf{X}_i$ and as well as vectors of strategies $\mathbf{S}_i$ are initialized by random values and initial values of masses is taken to be $2M_{\rm d}$. Simulations have been carried out for the values of parameters listed in Table 1.

One of the main purposes of the paper is to understand the impact of competition to the system dynamics. We decided to construct β-dependences of the mean statistical values. We start by rather artificial regime $\beta = 0$. In this trivially noncompetitive situation all masses attain $M_{\rm up}$ and optimization is equivalent to random walk. In Fig.(1)(a) we depict β-dependent effect of the competitive reduction of the

Symbol	Meaning	Value	Introduced
α	constant growth parameter	1.2	Eq.6
β	feedback parameter	varying	Eq.6
γ	exponent of interaction	4	Eq.8
ϵ	parameter of interaction	0.0005	Eq.8
N	number of agents	400	subsec.2.1
d_{x}	dimension of spatial coordinate	2	Eq.3
d_{s}	dimension of strategic variable	10	Eq.4
δ_{x_1}	small step of spatial optimization	0.01	subsec. 2.3
δ_{x_2}	long step of spatial optimization	0.2	subsec.2.3
δ_{s_1}	small step of strategy optimization	0.003	subsec.2.3
δ_{s_2}	long step of strategy optimization	0.03	subsec.2.3
J	interaction strength controller	1	Eq.8
L	square segment length	4	Eq.3
M_{d}	lower threshold for agent mass	0.02	subsec.2.4
M_{up}	upper threshold for agent mass	100	subsec.2.4
P_{big}	selection probability of bigger steps	0.2	subsec.2.3
P_{ps}	probability of decision to optimize	0.3	subsec.2.3

Table 1
Numerical values of model parameters used in the simulations supplemented by the short explanation and link to the main text where the issue is introduced.

mean mass $\langle M \rangle$, where $\langle \ldots \rangle$ stands for the numerical averaging over the time and assembly of the agents.

More profound picture of the system behavior is achieved by analyzing the statistics of mass fluctuations. The mass fluctuations around the mean $\langle M \rangle$ are characterized by the mass dispersion $\sigma^2_{\mathrm{M}} = \langle M^2 \rangle - \langle M \rangle^2$ [see Fig.2(a)]. The dependence of σ^2_{M} exhibits extreme at $\beta = \beta_{\mathrm{c}} = 1.2 \times 10^{-5}$. The value may be interpreted as the *critical point* of the phase transition driven by β. This scenario is consistent with the behaviour of the corresponding derivatives shown in insets of Fig.(1). The critical point separates phases of different competition (HCP and LCP, respectively). The phases were named according behavior of $\langle \Omega \rangle$ [Fig.1(b)]. For higher β we observed better (better in a sense of smaller $\langle \Omega \rangle$) way to minimize Ω_i that agents of HCP become self-improved because of more carefully chosen strategies.

The power-law distributions are assumed to be the hallmarks of criticality [33]. It is therefore instructive to identify the specific features of distributions regard-

ing position of critical point. The mass distributions have been studied for three representative β values: $\beta = 0.1\beta_{\rm c}$, $\beta_{\rm c}$, $10\beta_{\rm c}$ [see Fig. (3)]. Despite significant distance from the critical regime we see that distributions may be roughly characterized by the power-law distributions with anomalies concentrated around the tails of high and low mass regions. The parametric robustness of the power-law like distributions may be considered as realistic feature of the model. It is reasonable to suppose that anomalies originate prevailingly from the mass constraints (see subsec. 2.4). In our relatively small-size system the transition is not sharp but broad in β. Also performed detailed analysis of exponents ensures parametric robustness. To characterize the distributions more quantitatively, the respective M dependence of effective local index $\nu_{\rm eff}(M, \delta M)$ has been calculated for each of them. These dependences have been constructed by fitting of power-law functions of some exponent and amplitude on $(-\delta M + M, M + \delta M)$ for varying central M. Any plateau of $\nu_{\rm eff}(M, \delta M)$ indicates the existence of particular power-law behavior on the domains larger than δM. It should be noted that our idea of usage of local fits has been motivated by the phenomenology [34,35]. From the results obtained for different β we see that formation of power-law ditribution exhibits strong robustness with respect to $\beta_{\rm c}$ in the sense that particular local intervals of the power-law behavior stay sufficiently far from $\beta_{\rm c}$. On the other hand, the classical concept of the phase transition expresses itself through minimum spread of $\nu_{\rm eff} \simeq 0.19 - 0.31$ at the critical point.

In the following we supplement our optimization results with the information about transport properties. The diffusion coefficient is an indirect characteristics which is related to the spatial individual optimization. Its definition

$$D = \frac{1}{N} \sum_{i=1}^{N} \langle \parallel \mathbf{X}_i^{(t+\tau)} - \mathbf{X}_i^{(t)} \parallel^2 \rangle_{(\tau)} \tag{14}$$

captures space and time averaging of pathways. The index (τ) used to highlight data has been averaged over the time scale on the sub-assembly of the agents which live longer than τ. The above mentioned averages are depicted in Fig.(1)(d). They indicate that HCP agents spread faster owing to reduced interactions, caused by their reduced mass, abating blocking from the rivals.

The short-time efficiency of the optimization processes is analyzed using the fitness [36] function defined by the difference

$$\Delta\Omega_i^{(t)} = \Omega(\mathbf{X}_{i,(N_{\rm H})}^{(t)}, \mathbf{S}_i^{(t)}) - \Omega(\mathbf{X}_{i,(0)}^{(t)}, \mathbf{S}_i^{(t)}) \, . \tag{15}$$

(The same differences have been calculated and averaged when the optimization of strategy vectors is considered.) According to the above measure, the optimization of the position or strategy is more efficient if the difference becomes higher. But the difference measure tells little about the long-time perspectives of the agents.

Namely at HCP the landscape varies very rapidly and optimization yields only the short-time benefits from the movement. In the conditions of critical regime [see Fig.(2) (b)] the mean $\langle \Delta\Omega \rangle$ shows minimum. This confirms known fact that critical landscapes are landscapes of the extremal complexity [37,9].

The life expectancy characteristics depicted in Fig.(1)(c) indicates that the mean lifespan of HCP agents is considerably shorter in comparison with LCP agents. The combination of the above facts clearly indicates how inefficient the short-time optimization without prediction could be, namely in HCP constrictive conditions. The effect of enhanced diffusion as well as the effect of shortened life expectancy of agents could be considered as a typical examples of emergence, which has not been a priory integrated into the architecture of agents.

Finally our study has been focused on the mean individual growth of the agent as a function of his lifespan. The dependences depicted in Fig.(4) demonstrate saturation in qualitative agreement with the previously mentioned logistic forms. The analysis shows that despite the typically nonequilibrium nature of growth models, due to the projection of the mass into individual lifespan coordinate (and subsequent averaging over the assembly of masses belonging to the respective age), the mean growth dependences may be identified in the steady-state. For such numerical output, the carrying capacity can be identified a posteriori. Since agents often imitate mutually destructive and self-destructive actions, it seems rather surprising that saturation without recession appears at large lifespans. The qualitative microexplanation is that the drop of the mass of some agents is often accompanied by empowered growth of their respective neighbors and thus finally low-rate growth stem from the most of the rivalry crowds.

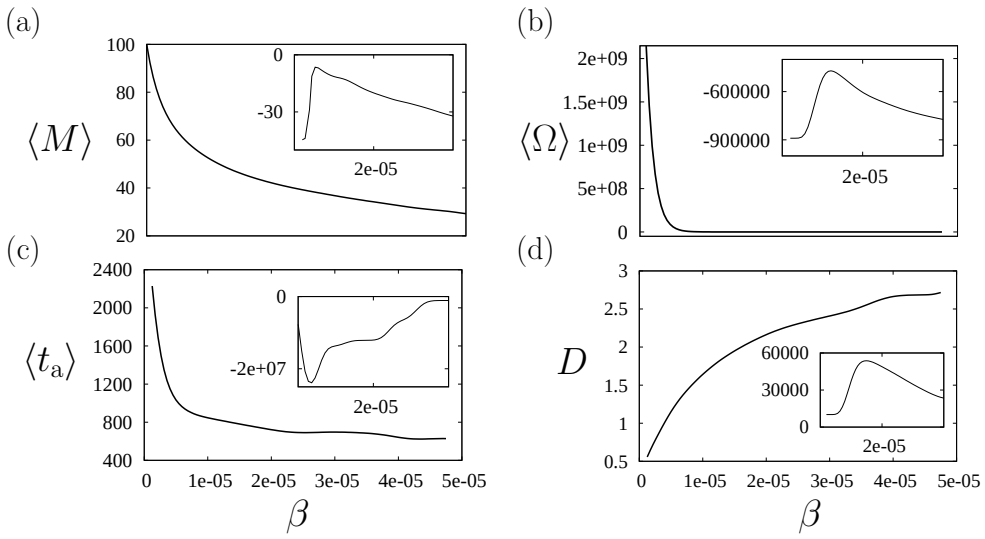

Fig. 1. The mean equilibrium characteristics in LCP and HCP phases plotted as a functions of the parameter β. The partial figures depict information about the mean: (a) *agent's mass* $\langle M \rangle$; (b) *mutual overlap* $\langle \Omega \rangle$ (match of strategies weighted by distance of agents); (c) *life expectancy* $\langle t_a \rangle$ reduced by competition at high β; (d) *diffusion coefficient* D showing enhanced migration effect when the competition gets more intense. Each part of figure is supplemented by the inset showing how the first derivative of the corresponding quantity changes with respect to β. All the anomalies are localized near the expected critical point. The main drawbacks here are the differences caused by the finite size effects. The dependences have been obtained by averaging of 13 independent runs going from the low to high β. For each run and each fixed β we treated record of data corresponding to 40 000 random visits per agent.

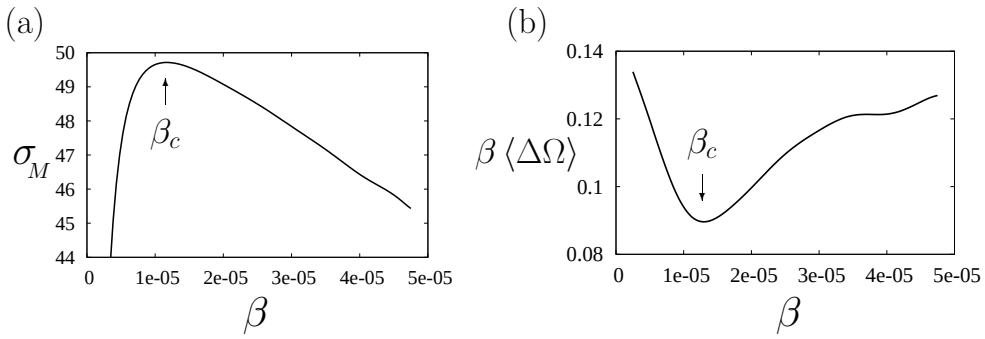

Fig. 2. The study of the fluctuations and their anomalies. The parts of figure include: (a) *mass dispersion* σ_{M}; (b) the measure of benefits $\langle \Delta\Omega \rangle$ that are gained by the short-time optimization. The extremes serve to identify critical point β_{c}.

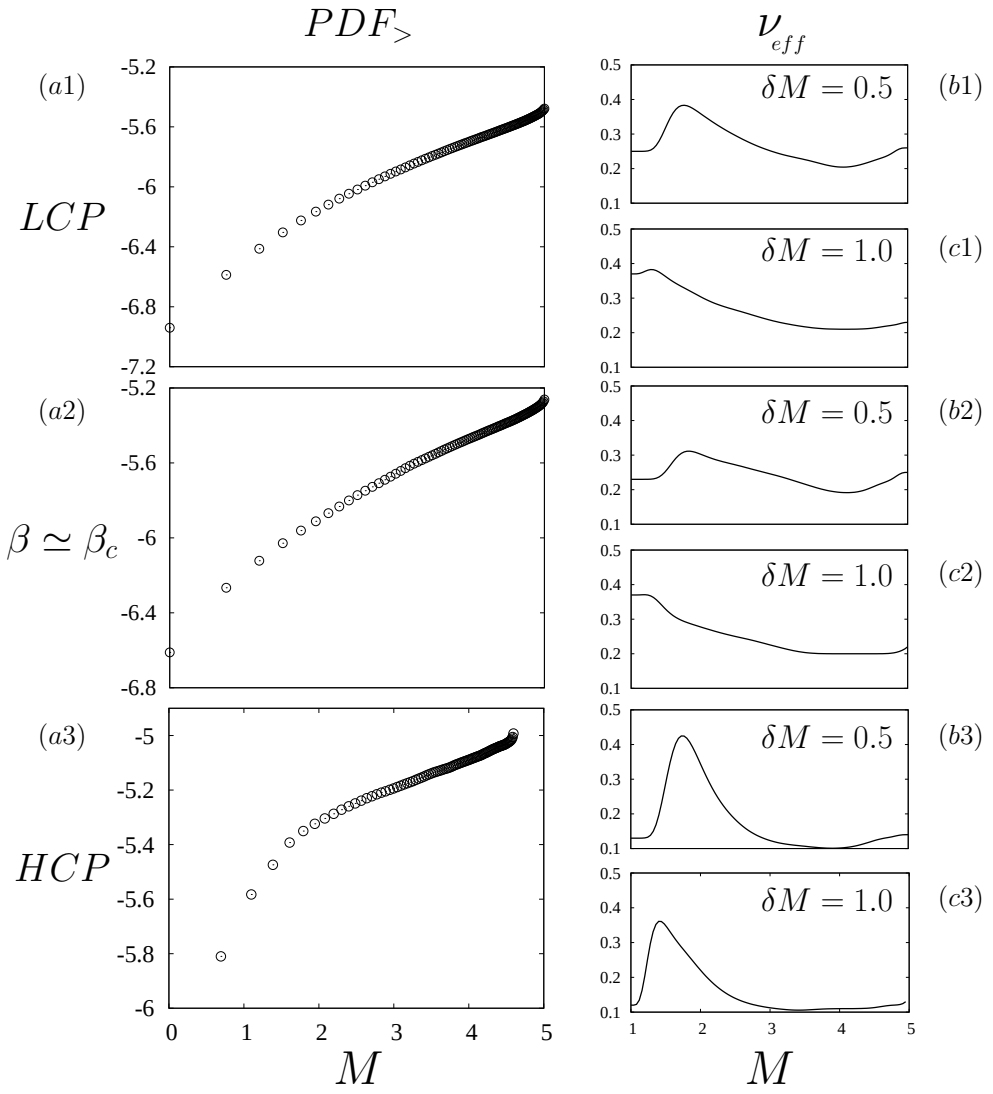

Fig. 3. The cumulative probability distributions and corresponding effective exponents (right hand side plots). Calculated for simulation data obtained for three representative values of β: (a1) $\beta = \beta_c/10$, (a2) $\beta = \beta_c$ and (a3) $\beta = 10\beta_c$. The local properties of distributions characterized by the effective exponent ν_{eff} which is a function of M (M is always middle point of the local fit) for two different resolutions δM. For $\delta M = 0.5$ and corresponding β we found that: (b1) $\nu_{\text{eff}} \in (0.2, 0.38)$; (b2) $\nu_{\text{eff}} \in (0.2, 0.31)$; (b3) $\nu_{\text{eff}} \in (0.1, 0.42)$. It means that the lowest spread of local effective exponent (b2) corresponds to the critical regime.

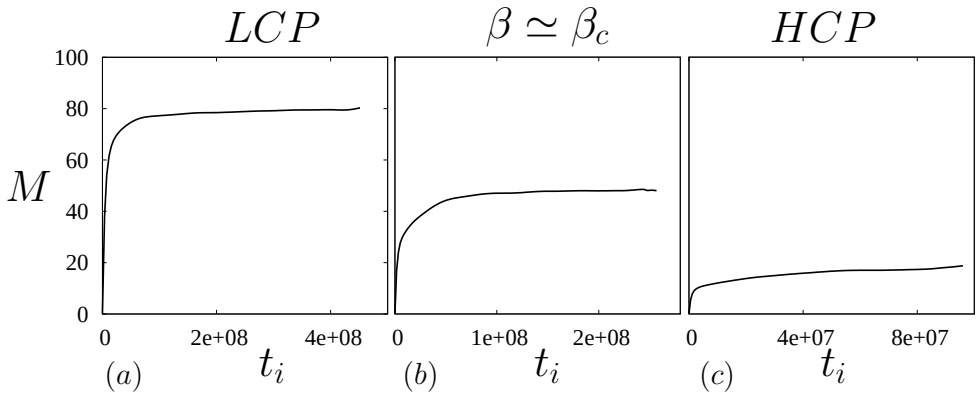

Fig. 4. The return to primary motivation for the model construction [see Eq.(1)]. The parts showing the individual mean mass growth as a function of the lifespan of agents. Each age group is averaged separately. Growth dependence is calculated for three representative values of β corresponding to: (a) LCP phase, ($\beta = \beta_{\rm c}/10$); (b) critical regime; (c) HCP phase, ($\beta = 10\beta_{\rm c}$).

4 Conclusion

In the paper the agent-based model of competitive behavior with implemented procedure of individual optimization was investigated. Our study focused on the equilibrium statistics and efficiency of the individual optimization. The principal finding is that there exists critical regime which indicates transition from the LCP to HCP phase and that there are significant differences in the efficiency of optimization in the respective phases. In HCP the low order resources are turned to the strategically well organized matter. The anomaly in the efficiency belongs to the complex barriers of Ω_i corresponding to critical point. We observed nearly power-law behavior of the mass distributions robust with respect to parametric choices. The focus on the tails of mass distributions suggests nonequivalence of central and close to boundary space positions, which cause nonuniform access to the external sources.

Among the emergent phenomena, which typically accompany the agent-based simulations, we could mention higher mobility of lighter agents and lifespan reduced by their motion close to lower mass region. In the future studies we plan to investigate the impact of an extra payoffs for the optimization and mobility which may strengthen competetivness.

In the paper we present results of the equilibrium simulations of the growth. As the equilibrium conditions are not always suitable for the growth problems, further perspectives of given model can be seen in nonequilibrium applications (e.g. in the models of metastatic growth with dissemination of malignant cells). It would be also interesting to combine individualized distributed parameters, e.g. those for decision to optimize (agent-dependent, distributed $P_{\mathrm{ps},i}$ instead of uniform P_{ps}), and analyze their impact on the mass statistics. Further perspectives can be seen in the application of the realistic geografic boundary conditions, space-distributed sources $\alpha(\mathbf{x})$ and assortment related to the specific sources.

Acknowledgements

The authors acknowledge financial support from VEGA, Slovak Republic (Grant No. 1/4021/07). One of the authors, D.H. acknowledges nancial support by a postdoctoral fellowship LESTUDIUM of the Region Centre and the Centre National de la Recherche Scientique (during his stay at the CBM and MAPMO CNRS institutes).

References

[1] P. Caplat, M. Anand, C. Bauch, Symmetric competition causes population oscillations in an individual-based model of forest dynamics, Ecol. Model. 211 (3-4) (2008) 491 – 500.

[2] J. Murray, Mathematical Biology I. An Introduction, Springer, 2001.

[3] G. Yaari, A. Nowak, K. Rakocy, S. Solomon, Microscopic study reveals the singular origins of growth, Eur. Phys. J. B 62 (4) (2008) 505–513.

[4] F. Webb, Theory of Nonlinear Age-dependent Population Dynamics, CRC Press, 2001.

[5] B. P. Ayati, G. F. Webb, A. Anderson, Computational methods and results for structured multiscale models of tumor invasion, Multiscale modeling and simulation 5 (2006) 1.

[6] Y. Mansury, T. S. Deisboeck, The impact of search precision in an agent-based tumor model, J. Theor. Biol. 224 (3) (2003) 325 – 337.

[7] A. Dasci, G. Laporte, A continuous model for multistore competitive location, Oper. Res. 53 (2) (2005) 263–280.

[8] T. Tabuchi, Two-stage two-dimensional spatial competition between two firms, Regional Science and Urban Economics 24 (2) (1994) 207–227.

[9] M. H. Chang, J. J. Harrington, Agent-based models of organizations, in: Handbook of Computational Economics, Vol. 2 of Handbook of Computational Economics, Elsevier, 2006, Ch. 26, pp. 1273–1337.

[10] E. Bonabeau, Agent-based modeling: Methods and techniques for simulating human systems, Proc. Natl. Acad. Sci. USA 99 (Suppl 3) (2002) 7280–7287.

[11] V. A. Cicirello, S. F. Smith, Insect societies and manufacturing, in: In IJCAI-01 Workshop on Artificial Intelligence and Manufacturing: New AI Paradigms for Manufacturing, 2001, pp. 328–9.

[12] W. Xiang, H. P. Lee, Ant colony intelligence in multi-agent dynamic manufacturing scheduling, Eng. Appl. Artif. Intell. 21 (1) (2008) 73–85.

[13] Y. Sunitiyoso, S. Matsumoto, Modelling a social dilemma of mode choice based on commuters' expectations and social learning, Eur. J. Oper. Research 193 (3) (2009) 904 – 914.

[14] W. Cook, P. Ormerod, Power law distribution of the frequency of demises of US firms, Physica A 324 (1-2) (2003) 207 – 212.

[15] J. P. Bouchaud, M. Mezard, Wealth condensation in a simple model of economy, Physica A 282 (2000) 536–545.

[16] H. Aoyama, Y. Fujiwara, W. Souma, Kinematics and dynamics of Pareto-Zipf's law and gibrat's law, Physica A 344 (1-2) (2004) 117 – 121.

[17] A. Chatterjee, B. K. Chakrabarti, S. S. Manna, Money in gas-like markets: Gibbs and pareto laws, Phys. Scr. T106 (2003) 36–38.

[18] Y. Fujiwara, H. Aoyama, C. Guilmi, W. Souma, M. Gallegati, Gibrat and pareto-zipf revisited with european firms, Physica A 344 (1-2) (2004) 112 – 116.

[19] R. Stanley, S. V. Buldyrev, S. Havlin, R. N. Mantegna, M. A. Salinger, H. E. Stanley, Zipf plots and the size distribution of firms, Econ. Lett. 49 (4) (1995) 453 – 457.

[20] M. L. Palima, E. J. David, Wealth distribution in a system with wealth-limited interactions, arXiv:q-fin.GN/0710.1014v1.

[21] K. L. Judd, Optimal taxation and spending in general competitive growth models, J. Pub. Econ. 71 (1) (1999) 1–26.

[22] V. Pareto, Cours d' Economique Politique, Macmillan, 1897.

[23] E. H. Decker, A. J. Kerkhoff, M. E. Moses, Global patterns of city size distributions and their fundamental drivers, PLoS ONE 2 (9) (2007) 934.

[24] P. A. Rikvold, Self-optimization, community stability, and fluctuations in two individual-based models of biological coevolution, J. Math. Biol. 55 (2007) 653–677.

[25] Z. Olami, H. J. S. Feder, K. Christensen, Self-organized criticality in a continuous, nonconservative cellular automaton modeling earthquakes, Phys. Rev. Lett. 68 (1992) 1244–1247.

[26] A. Manor, N. M. Shnerb, From companies to colonies: The origin of pareto-like distributions in ecosystems, arXiv:q-bio.PE/0810.0841v1.

[27] J. Bechhoefer, Feedback for physicists: A tutorial essay on control, Rev. Mod. Phys. 77 (2005) 783–836.

[28] P. Bak, C. Tang, K. Wiesenfeld, Self-organized criticality, Phys. Rev. A 38 (1) (1988) 364–374.

[29] D. Horváth, M. Gmitra, Z. Kuscsik, A self-adjusted Monte Carlo simulation as a model for financial markets with central regulation, Physica A 361 (2006) 589–605.

[30] C. O. Wilke, C. Ronnewinkel, T. Martinetz, Dynamic fitness landscapes in molecular evolution, Phys. Rep. 349 (2001) 395–446.

[31] K. Painter, J. A. Sherratt, Modelling the movement of interacting cell populations, J. Theor. Biol. 225 (3) (2003) 327 – 339.

[32] G. Wit, Firm size distributions: An overview of steady-state distributions resulting from firm dynamics models, Int. J. of Ind. Organ. 23 (5-6) (2005) 423 – 450.

[33] M. E. J. Newman, Power laws, Pareto distributions and Zipf's law, Contemp. Phys. 46 (2005) 323.

[34] R. Coelho, P. Richmond, J. Barry, S. Hutzler, Double power laws in income and wealth distributions, Physica A 387 (15) (2008) 3847 – 3851.

[35] A. Scarfone, A mechanism to derive multi-power law functions: An application in the econophysics framework, Physica A 382 (1) (2007) 271 – 277.

[36] G. S. G. Beveridge, R. S. Schechter, Optimization: Theory and Practice, McGraw-Hill, 1970.

[37] C. G. Langton, Computation at the edge of chaos: Phase transitions and emergent computation, Physica D 42 (1990) 12–37.